Markedly Reduced Apparent Blood Volume on Bolus Contrast Magnetic Resonance Imaging as a Predictor of Hemorrhage After Thrombolytic Therapy for Acute Ischemic Stroke

David C. Alsop, PhD; Elena Makovetskaya, BS; Sandeep Kumar, MD;
Magdy Selim, MD, PhD; Gottfried Schlaug, MD, PhD

Background and Purpose—Accurate assessment of the risk of hemorrhage could help to improve patient selection for thrombolytic therapy and reduce hemorrhagic complications, especially for patients with longer or uncertain time after symptom onset. This study sought to define characteristics of hemodynamic magnetic resonance imaging (MRI), which best predict hemorrhage.

Methods—Bolus contrast and diffusion MRI were performed before intravenous tissue plasminogen activator (tPA) therapy in 20 patients presenting with acute stroke symptoms within the first 6 hours after symptom onset. Hemorrhage was assessed on follow-up MRI (n=15) and computed tomography (n=5) scans.

Results—Of the 20 patients studied, 5 had detectable hemorrhage on follow-up scans. Blood volume maps demonstrated virtually no signal within much of the hemorrhagic region, indicating contrast did not arrive by the end of the imaging series (80 seconds). Within the hemodynamically abnormal region, a threshold of at least 126 voxels with blood volume <5% of contralateral normal gray matter separated hemorrhagic patients from nonhemorrhagic with a sensitivity of 100% and a specificity of 73% ($P<0.01$). All subjects with hemorrhage were at least partially reperfused after thrombolysis, whereas most false-positives did not reperfuse ($P<0.05$). The number of low blood volume voxels within individual patients correlated with the number of voxels with apparent diffusion coefficient values $<550\times10^{-6}$ mm^2/s ($P<0.019$), another previously proposed predictor of hemorrhage.

Conclusions—Extremely low or completely absent contrast arrival may indicate tissue-at-risk for hemorrhage before tPA treatment and thus may aid in risk–benefit assessments. Occurrence of hemorrhage within at-risk areas may depend on tissue reperfusion. (***Stroke***. 2005;36:746-750.)

Key Words: hemodynamics ■ hemorrhage ■ magnetic resonance imaging ■ thrombolytic therapy

Thrombolysis-induced reperfusion is a proven therapy for acute ischemic stroke when performed within the first few hours after symptom onset.[1,2] On average, the benefit of thrombolysis fades with time[3,4]; however, the risk of cerebral hemorrhage remains constant or increasing.[1,5] Severe hemorrhage can cause worsening of stroke symptoms, whereas smaller hemorrhages may negate much of the potential benefit of reperfusion. Concern for hemorrhage risk is the primary reason for the use of time windows to constrain the treatment with thrombolysis to those patients for whom the risk-to-benefit ratio is most favorable.[5] In addition to delay time, size of the initial ischemic lesion has been associated with increased risk for post-treatment hemorrhage[6] and has been used as an exclusion criterion. With additional information, the risk and benefit of thrombolysis for individual patients may differ significantly from the mean of the entire acute stroke population such that

reperfusion at later time points or in patients for whom the time of onset is not well known may be indicated.

Imaging can provide patient specific information on the risk and benefit of thrombolytic therapy.[7–11] X-ray computed tomography (CT) or potentially magnetic resonance imaging (MRI) is already required to rule out the occurrence of hemorrhage before thrombolysis with tissue plasminogen activator (tPA). The mismatch between the size of the initial ischemic lesion with diffusion MRI and the presence and size of a surrounding hypoperfused region as determined with dynamic susceptibility contrast (DSC) has been used as an indicator of the potential benefit of reperfusion therapy.[12] Similar approaches using CT[13] and positron emission tomography[14] have been investigated.

An imaging method for the prediction of hemorrhage after thrombolysis-induced reperfusion would greatly alter the deci-

© 2005 American Heart Association, Inc.

Stroke is available at http://www.strokeaha.org

DOI: 10.1161/01.STR.0000158913.91058.93

sion process for treatment. Though hemorrhage after tPA administration can sometimes occur outside of the ischemic region,[15] hemorrhage occurs predominantly within the ischemic lesion. Hemorrhage within the core of the stroke is most likely related to the duration and severity of the ischemia.[16,17]

Severe ischemia as indicated by the quantitative value of the MRI-measured apparent diffusion coefficient (ADC) has been shown to have predictive power for hemorrhagic transformation.[7–11] Diffusion is, however, primarily a characteristic of the tissue rather than the microvasculature, whose damage ultimately causes hemorrhage.[18] The quantitative ADC is a function of perfusion and time[19] that may differ from the response of the underlying microvasculature. ADC also can only be measured by MRI, which may not be available for all clinical and research studies. Studies using SPECT as an indicator of blood flow have demonstrated a correlation between very low blood flow and hemorrhage after thrombolytic therapy.[17,20–23] Here, we examine hemodynamic correlates of hemorrhage risk after thrombolytic therapy as measured with DSC MRI.

Subjects and Methods

Patients were selected retrospectively over the past 4 years from a prospectively collected stroke database. We identified patients treated with intravenous tPA for ischemic stroke within 6 hours of symptom onset with acceptable-quality DSC MRI scans before treatment and diagnostic-quality MRI (n=15) or CT (n=5) scans within 1 to 5 days after treatment. Most patients in the database were excluded because of the lack of a DSC study at the initial time point. Patients from the 3- to 6-hour time window were part of 2 approved experimental protocols using intravenous tPA. Twenty subjects were identified fulfilling the criteria. All subjects were studied using procedures approved by our medical center's institutional review board.

Imaging

All patients were imaged using a standardized stroke imaging protocol, whose details are described elsewhere.[10,24,25] Perfusion imaging used gradient echo echoplanar imaging with a echo time of 50 ms repeated every 2 seconds for up to 80 seconds. The bolus of 0.1 mmol/kg Gd-DTPA followed by 20 mL normal saline was injected after the fourth acquisition. Between 12 and 20, 7-mm-thick slices were acquired with an in plane resolution of 2×2 mm. Hemorrhage on the follow-up scan was detected by experienced neuroradiologists using susceptibility-sensitive MRI or X-ray CT.

Intravenous tPA was administered according to standard guidelines. Success of reperfusion was inferred from Doppler ultrasound, follow-up perfusion MRI or magnetic resonance angiography, and/or change in the hyperdense middle cerebral artery signs on noncontrast CT (n=1).

Image Processing

DSC images were corrected for motion using a 2-step process. First, the subsequent images were aligned to the first image using an iterative simplex algorithm and a rigid body rotation model. After this alignment, the logarithm of the images was calculated and then the images were separated into independent components using an implementation of the infomax algorithm.[26,27] Independent components could readily be separated into motion-related and contrast-related components by visual assessment of the spatial distribution and temporal response. Contrast-related components were selected and recombined to provide more accurate time series data.

The DSC times series were converted into quantitative images of mean transit time (MTT), relative cerebral blood flow, and relative cerebral blood volume using a nonlinear least square fitting approach and an input function selected from the images using a minimum first moment criterion. Accurate quantification of MTT in the presence of delay and spreading of the bolus caused by stenosis and collateral flow
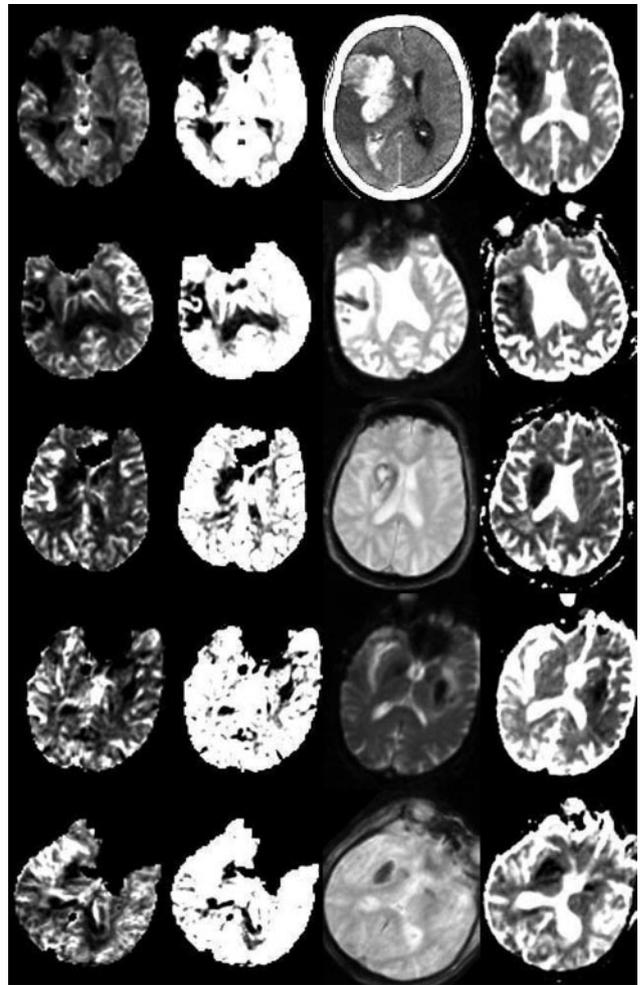
Figure 1. Comparison of acute aCBV and ADC maps with hemorrhage location on follow-up scans in the 5 patients with hemorrhage. aCBV is shown at 2 different window levels, left 2 columns, for comparison with the hemorrhage as shown on susceptibility or CT follow-up imaging, third row. Acute ADC maps are shown in the rightmost column.

is still an active area of development.[28] Hemorrhage prediction focused on the cerebral blood volume maps. Because cerebral blood volume maps underestimate blood volume in regions of very slow or delayed inflow,[24,29] they are referred to as apparent cerebral blood volume (aCBV).

Quantitative ADC values were derived from the diffusion imaging using standard methods.[30,31] ADC images were aligned to the DSC hemodynamic images using an iterative simplex algorithm and a rigid body rotation model because the patients sometimes moved between diffusion and bolus contrast scans.

Regions of interest were manually drawn on the MTT maps to grossly define the hemodynamically abnormal area. Because ventricles and other cerebrospinal fluid (CSF)-filled spaces have low blood volume and noisy MTT, we removed voxels containing primarily cerebrospinal fluid. These voxels were identified by their strong signal decrease from the first to second image in the time series.

Results

After tPA therapy, 5 of the 20 patients had hemorrhagic signatures on their follow-up images. Analysis of the perfusion images showed that severely reduced aCBV was apparent within each of the regions that eventually bled (Figure 1). In contrast, the MTT maps showed large variations across the
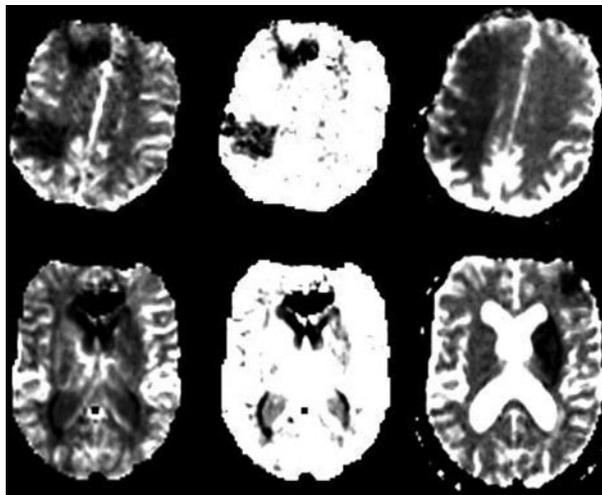
Figure 2. Comparison of acute aCBV and ADC maps in 2 patients without subsequent hemorrhage. aCBV is shown at 2 different window levels, left 2 columns. Acute ADC maps are shown in the rightmost column. The patient in the upper row shows both very low aCBV and ADC but without subsequent hemorrhage. The patient in the lower row shows very low ADC but only slight reduction of aCBV.

Figure 3. Receiver operating characteristic (ROC) curves for the assessment aCBV and ADC as predictors of hemorrhage. Sensitivity and specificity were determined as the criterion on the number of aCBV or ADC voxels above threshold was raised from 0 to above the largest number observed.

region of aCBV abnormality. Measurement of MTT requires the passage of a detectable bolus within the imaging period; when there is no bolus arrival, the MTT calculations will produce spurious results and will appear noisy. Thus, the very noisy MTT combined with the low aCBV are consistent with the absence of detectable contrast arrival within the region destined for hemorrhage.

Severe reduction of ADC also appeared spatially correlated with hemorrhage and consequently the regions of severely reduced aCBV. Representative slices from each of the 5 subjects are compared in Figure 1. Despite the excellent agreement between the 2 techniques and the location of hemorrhage, agreement was not perfect within the nonhemorrhagic group (Figure 2).

Numbers of voxels below the aCBV (5% of contralateral normal region of interest) or ADC ($<550 \times 10^{-6}$ mm^2/s) thresholds within the MTT abnormal region were calculated for each subject. All of the subjects, even those who did not bleed, had at least a few voxels within the MTT abnormality that were below each of the thresholds. Not all of the voxels had any biological or clinical meaning. Some of these voxels were small clusters near edges where motion adds extra noise or in deep white matter where blood volume is normally lower and noise or small amounts of motion can push the values below threshold.

The number of voxels with subthreshold aCBV values was significantly higher in the hemorrhage group than the nonhemorrhage group (Mann–Whitney $P<0.03$; Table). The number of voxels with subthreshold ADC values was not significantly different between the groups (Mann–Whitney $P=0.52$). Although 1 subject was dropped from the diffusion analysis because of poor diffusion image quality, the group difference for the number of aCBV voxels remained significant without this subject ($P<0.033$). The number of voxels below threshold for aCBV and ADC were significantly correlated in the 19 subjects with diffusion data. Several clinical factors including acute National Institutes of Health
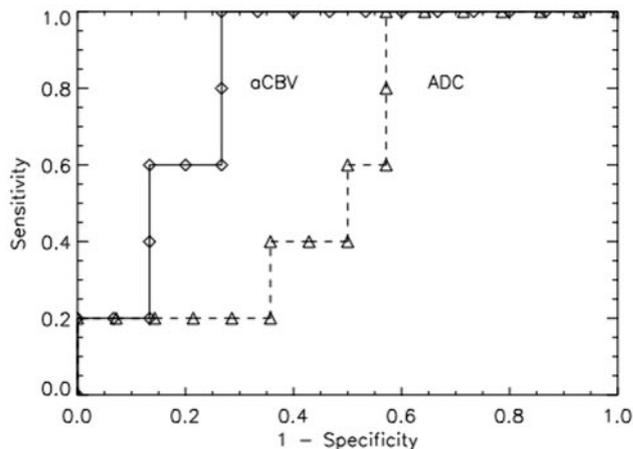
Stroke Scale score, MTT lesion size, and time of onset were also significantly correlated with aCBV voxel number. No single factor besides aCBV voxel number was a significant univariate predictor of hemorrhage, however.

In the next step, we assessed subthreshold voxel numbers as a predictive marker for hemorrhage. Receiver operating characteristic curves for both aCBV and ADC are shown in Figure 3. The aCBV receiver operating characteristic curve had superior sensitivity for any specificity and consequently the area under the receiver operating characteristic curve, an indicator of diagnostic power, was higher for aCBV. A cutoff of 126 voxels with subthreshold aCBV was selected to minimize false-negatives. This threshold predicts all 5 hemorrhages (100% sensitivity) with 4 false-positives (73% specificity) and 11 true negatives ($P<0.01$ Fisher exact test). Reperfusion was significantly different between the 5 true positives (all at least partially reperfused) and the 4 false-positives (3 did not reperfuse; 1 partially reperfused; Fisher exact test $P<0.05$).

Finally, we assessed the effect of different aCBV thresholds on specificity. Thresholds from 0.5% to 50% of contralateral gray matter were chosen and the voxel number cutoff that gave the maximum specificity at 100% sensitivity was selected. The corresponding specificity is shown in Figure 4. Peak specificity occurred between 1.5 and 13% thresholds. The falloff of specificity with increasing threshold, and corresponding optimal voxel number cutoff, indicates that the magnitude and not the size of the aCBV abnormality is the important diagnostic factor.

Discussion

These results support the hypothesis that post-thrombolytic hemorrhage is related to severe ischemia. This severe level of ischemia is apparent in standard bolus contrast studies as a failure of contrast arrival within the tissue. Quantitative analyses that calculate time-to-peak, MTT, or blood flow will fail in regions without contrast arrival because of their inherent dependence on a changing contrast concentration over time. Thus, we propose apparent CBV as a simple and reliable indicator of severe ischemia and post-thrombolytic hemorrhage risk.
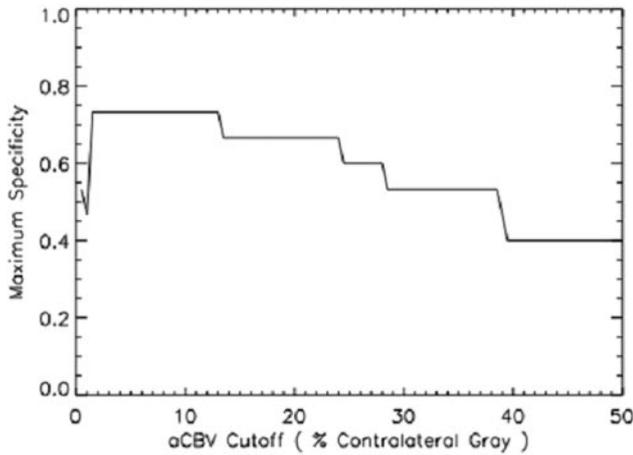
Figure 4. Maximum specificity obtained using different aCBV thresholds to predict hemorrhage. The voxel number cutoff at each aCBV threshold was adjusted to achieve 100% sensitivity with maximum specificity. Specificity was optimal for a low aCBV threshold emphasizing the importance of severe ischemia in inducing hemorrhage.

Because contrast typically arrives within the normal brain in ≈1 second, the failure to detect contrast arrival in >1 minute of acquisition suggests a local blood flow reduction to <2% of normal. This level of flow is far below the threshold for irreversible ischemic damage to tissue but may represent an ischemic threshold for the microvasculature. Alternatively, such low flow may indicate constriction of the microvasculature after energetic failure at an initially higher flow level. Decreasing blood volume over time with severe ischemia has been shown in a rat model of stroke.[32]

Although the spatial overlap between the locations of negligible aCBV and eventual hemorrhage appears compelling, almost as many subjects with the extremely low aCBV signature did not hemorrhage. In our limited sample, hemorrhage occurred exclusively in patients with at least partial reperfusion. Only 1 of the 4 subjects demonstrating the extremely low aCBV signature but without subsequent hemorrhage reperfused. This subject demonstrated the low aCBV (before thrombolytic therapy) in the superior borderzone region between the anterior cerebral artery and middle cerebral artery territories (Figure 2, top). Because reperfusion in the follow-up imaging study was only assessed until slightly above the circle of Willis, there is a possibility that

this patient was not completely reperfused because distal branches of the middle cerebral artery and anterior cerebral artery supplying the watershed territory were not fully imaged. Because tPA administration increases the rate of reperfusion and also the risk of hemorrhage, reperfusion of severely ischemic regions is a plausible requirement for hemorrhagic transformation. However, direct effects of tPA on blood vessels may play a role in hemorrhagic transformation,[18,33] as well as other patient-dependent risk factors such as serum glucose levels.[10,34,35] A larger sample size will be required to assess the relationship between our aCBV indicator, reperfusion, lesion location, and patient-dependent risk factors.

In this sample, aCBV outperformed ADC as a predictor of hemorrhage. This lower predictive power of ADC may be related to differences in the response of tissue and microvasculature to the severity and duration of ischemia. Hemorrhage risk assessment by aCBV has the added advantage that it may also be possible using imaging modalities other than MRI, such as contrast CT,[36] although a similar hemorrhage risk analysis has yet to be performed.

Whereas aCBV was found to be a useful indicator of hemorrhage risk, the effect and clinical significance of smaller, asymptomatic hemorrhage on outcome after thrombolysis is uncertain. Blood products can have toxic effects on the brain,[37] but these effects may not negate the positive effects of reperfusion to a larger volume.[38] Two of the asymptomatic hemorrhage cases in our study showed clinical improvement at 24 hours. In our 5 hemorrhagic cases, the number of subthreshold aCBV voxels was higher in the 2 symptomatic hemorrhage cases compared with the 3 asymptomatic cases, but the limited sample size prevented a meaningful assessment of the predictive power for size or clinical severity of post-thrombolytic hemorrhage.

In conclusion, our results indicate that hemorrhage after tPA administration occurs in regions with very low aCBV on bolus contrast MRI studies. This indicator provided predictive power superior to quantitative ADC, at least within our sample, and also showed excellent spatial registration with the later hemorrhage. Reperfusion was significantly related to the occurrence of hemorrhage in those subjects with the extremely low aCBV signature. This indicator may help assess tissue at risk for hemorrhage after tPA treatment. The indicator might be particularly useful when treating patients beyond the 3-hour time window or when treating

Group Differences of Clinical and Imaging Parameters

	Hemorrhage Group (n=5)	Nonhemorrhage Group (n=15)	*P of Group Difference	†P of Correlation With No. of aCBV Voxels
Age, y (range)	76.6 (73–86)	71.5 (33–89)	0.793	0.816
% Female	20	47	0.603	
Acute NIHSS (range)	18.0 (14–22)	17.7 (7–42)	0.599	0.040
Onset time, min (range)	232 (150–357)	194 (111–380)	0.355	0.075
Glucose, mg/dL (range)	164 (115–267)	121 (87–182)	0.097	0.237
MTT size, mL (range)	144 (92–194)	177 (25–422)	0.631	0.029
No. of ADC voxels‡ (range)	286 (113–1124)	252 (1–852)	0.578	0.019
No. of aCBV voxels (range)	565 (127–2271)	202 (2–1100)	0.026	

*Mann–Whitney test, 2-tailed.

†Spearman rank correlation, 2-tailed.

‡One subject from the nonhemorrhage group was not included because of absence of diffusion imaging of sufficient quality.

patients with unknown time of onset,[25] because risk for hemorrhage is typically the highest concern in these patient groups.

Acknowledgments

References

1. NINDS rt-PA Stroke Study Group. Tissue plasminogen activator for acute ischemic stroke. The national institute of neurological disorders and stroke rt-PA stroke study group. *N Engl J Med.* 1995;333:1581–1587.
2. Donnan GA, Davis SM, Chambers BR, Gates PC, Hankey GJ, McNeil JJ, Rosen D, Stewart-Wynne EG, Tuck RR. Streptokinase for acute ischemic stroke with relationship to time of administration: Australian streptokinase (ASK) trial study group. *JAMA.* 1996;276:961–966.
3. Marler JR, Tilley BC, Lu M, Brott TG, Lyden PC, Grotta JC, Broderick JP, Levine SR, Frankel MP, Horowitz SH, Haley EC, Jr., Lewandowski CA, Kwiatkowski TP. Early stroke treatment associated with better outcome: the NINDS rt-PA stroke study. *Neurology.* 2000;55:1649–1655.
4. Hacke W, Donnan G, Fieschi C, Kaste M, von Kummer R, Broderick JP, Brott T, Frankel M, Grotta JC, Haley EC, Jr., Kwiatkowski T, Levine SR, Lewandowski C, Lu M, Lyden P, Marler JR, Patel S, Tilley BC, Albers G, Bluhmki E, Wilhelm M, Hamilton S. Association of outcome with early stroke treatment: pooled analysis of ATLANTIS, ECASS, and NINDS rt-PA stroke trials. *Lancet.* 2004;363:768–774.
5. Clark WM, Wissman S, Albers GW, Jhamandas JH, Madden KP, Hamilton S. Recombinant tissue-type plasminogen activator (alteplase) for ischemic stroke 3 to 5 hours after symptom onset. The ATLANTIS study: a randomized controlled trial. Alteplase thrombolysis for acute noninterventional therapy in ischemic stroke. *JAMA.* 1999;282:2019–2026.
6. Larrue V, von Kummer RR, Muller A, Bluhmki E. Risk factors for severe hemorrhagic transformation in ischemic stroke patients treated with recombinant tissue plasminogen activator: a secondary analysis of the European-Australasian Acute Stroke Study (ECASS II). *Stroke.* 2001;32:438–441.
7. Tong DC, Adami A, Moseley ME, Marks MP. Prediction of hemorrhagic transformation following acute stroke: role of diffusion- and perfusion-weighted magnetic resonance imaging. *Arch Neurol.* 2001;58:587–593.
8. Tong DC, Adami A, Moseley ME, Marks MP. Relationship between apparent diffusion coefficient and subsequent hemorrhagic transformation following acute ischemic stroke. *Stroke.* 2000;31:2378–2384.
9. Adami A, Thijs V, Tong DC, Beaulieu C, Moseley ME, Yenari MA. Use of diffusion weighted MRI to predict the occurrence and severity of hemorrhagic transformation in a rabbit model of embolic stroke. *Brain Res.* 2002;944:32–39.
10. Selim M, Fink JN, Kumar S, Caplan LR, Horkan C, Chen Y, Linfante I, Schlaug G. Predictors of hemorrhagic transformation after intravenous recombinant tissue plasminogen activator: prognostic value of the initial apparent diffusion coefficient and diffusion-weighted lesion volume. *Stroke.* 2002;33:2047–2052.
11. Oppenheim C, Samson Y, Dormont D, Crozier S, Manai R, Rancurel G, Fredy D, Marsault C. Dwi prediction of symptomatic hemorrhagic transformation in acute MCA infarct. *J Neuroradiol.* 2002;29:6–13.
12. Albers GW. Expanding the window for thrombolytic therapy in acute stroke. The potential role of acute MRI for patient selection. *Stroke.* 1999;30:2230–2237.
13. von Kummer R, Bourquain H, Bastianello S, Bozzao L, Manelfe C, Meier D, Hacke W. Early prediction of irreversible brain damage after ischemic stroke at CT. *Radiology.* 2001;219:95–100.
14. Read SJ, Hirano T, Abbott DF, Sachinidis JI, Tochon-Danguy HJ, Chan JG, Egan GF, Scott AM, Bladin CF, McKay WJ, Donnan GA. Identifying hypoxic tissue after acute ischemic stroke using pet and 18f-fluoromisonidazole. *Neurology.* 1998;51:1617–1621.
15. Nighoghossian N, Hermier M, Adeleine P, Blanc-Lasserre K, Derex L, Honnorat J, Philippeau F, Dugor JF, Froment JC, Trouillas P. Old microbleeds are a potential risk factor for cerebral bleeding after ischemic stroke: A gradient-echo T2*-weighted brain MRI study. *Stroke.* 2002;33:735–742.
16. Dijkhuizen RM, Asahi M, Wu O, Rosen BR, Lo EH. Delayed rt-pa treatment in a rat embolic stroke model: diagnosis and prognosis of ischemic injury and hemorrhagic transformation with magnetic resonance imaging. *J Cereb Blood Flow Metab.* 2001;21:964–971.
17. Umemura A, Suzuka T, Yamada K. Quantitative measurement of cerebral blood flow by (99m)Tc-HMPAO SPECT in acute ischaemic stroke: use-
18. del Zoppo GJ, von Kummer R, Hamann GF. Ischaemic damage of brain microvessels: inherent risks for thrombolytic treatment in stroke. *J Neurol Neurosurg Psychiatry.* 1998;65:1–9.
19. Lin W, Lee JM, Lee YZ, Vo KD, Pilgram T, Hsu CY. Temporal relationship between apparent diffusion coefficient and absolute measurements of cerebral blood flow in acute stroke patients. *Stroke.* 2003;34:64–70.
20. Hanson SK, Grotta JC, Rhoades H, Tran HD, Lamki LM, Barron BJ, Taylor WJ. Value of single-photon emission-computed tomography in acute stroke therapeutic trials. *Stroke.* 1993;24:1322–1329.
21. Ueda T, Hatakeyama T, Kumon Y, Sakaki S, Uraoka T. Evaluation of risk of hemorrhagic transformation in local intra-arterial thrombolysis in acute ischemic stroke by initial SPECT. *Stroke.* 1994;25:298–303.
22. Alexandrov AV, Black SE, Ehrlich LE, Caldwell CB, Norris JW. Predictors of hemorrhagic transformation occurring spontaneously and on anticoagulants in patients with acute ischemic stroke. *Stroke.* 1997;28:1198–1202.
23. Ueda T, Sakaki S, Yuh WT, Nochide I, Ohta S. Outcome in acute stroke with successful intra-arterial thrombolysis and predictive value of initial single-photon emission-computed tomography. *J Cereb Blood Flow Metab.* 1999;19:99–108.
24. Schlaug G, Benfield A, Baird AE, Siewert B, Lovblad KO, Parker RA, Edelman RR, Warach S. The ischemic penumbra: operationally defined by diffusion and perfusion MRI. *Neurology.* 1999;53:1528–1537.
25. Fink JN, Kumar S, Horkan C, Linfante I, Selim MH, Caplan LR, Schlaug G. The stroke patient who woke up—clinical and radiological features, including diffusion and perfusion MRI. *Stroke.* 2002;33:988–993.
26. Bell AJ, Sejnowski TJ. An information maximization approach to blind separation and blind deconvolution. *Neural Computation.* 1995;7:1129–1159.
27. Amari S, Cichocki A, Yang HH. A new learning algorithm for blind signal separation. In: Touretzky D, Mozer M, Hasselmo M, eds. *Advances in Neural Information Processing Systems 8.* Cambridge, MA: MIT Press; 1996:757–763.
28. Calamante F, Gadian DG, Connelly A. Delay and dispersion effects in dynamic susceptibility contrast MRI: simulations using singular value decomposition. *Magn Reson Med.* 2000;44:466–473.
29. Perkio J, Aronen HJ, Kangasmaki A, Liu Y, Karonen J, Savolainen S, Ostergaard L. Evaluation of four postprocessing methods for determination of cerebral blood volume and mean transit time by dynamic susceptibility contrast imaging. *Magn Reson Med.* 2002;47:973–981.
30. van Gelderen P, de Vleeschouwer MH, DesPres D, Pekar J, van Zijl PC, Moonen CT. Water diffusion and acute stroke. *Magn Reson Med.* 1994;31:154–163.
31. Alsop DC. Phase insensitive preparation of single-shot rare: application to diffusion imaging in humans. *Magn Reson Med.* 1997;38:527–533.
32. Zaharchuk G, Yamada M, Sasamata M, Jenkins BG, Moskowitz MA, Rosen BR. Is all perfusion-weighted magnetic resonance imaging for stroke equal? The temporal evolution of multiple hemodynamic parameters after focal ischemia in rats correlated with evidence of infarction. *J Cereb Blood Flow Metab.* 2000;20:1341–1351.
33. Sumii T, Lo EH. Involvement of matrix metalloproteinase in thrombolysis-associated hemorrhagic transformation after embolic focal ischemia in rats. *Stroke.* 2002;33:831–836.
34. Kidwell CS, Saver JL, Carneado J, Sayre J, Starkman S, Duckwiler G, Gobin YP, Jahan R, Vespa P, Villablanca JP, Liebeskind DS, Vinuela F. Predictors of hemorrhagic transformation in patients receiving intra-arterial thrombolysis. *Stroke.* 2002;33:717–724.
35. Demchuk AM, Morgenstern LB, Krieger DW, Linda Chi T, Hu W, Wein TH, Hardy RJ, Grotta JC, Buchan AM. Serum glucose level and diabetes predict tissue plasminogen activator-related intracerebral hemorrhage in acute ischemic stroke. *Stroke.* 1999;30:34–39.
36. Hunter GJ, Silvennoinen HM, Hamberg LM, Koroshetz WJ, Buonanno FS, Schwamm LH, Rordorf GA, Gonzalez RG. Whole-brain ct perfusion measurement of perfused cerebral blood volume in acute ischemic stroke: probability curve for regional infarction. *Radiology.* 2003;227:725–730.
37. Bishop GM, Robinson SR. Quantitative analysis of cell death and ferritin expression in response to cortical iron: implications for hypoxia-ischemia and stroke. *Brain Res.* 2001;907:175–187.
38. Molina CA, Alvarez-Sabin J, Montaner J, Abilleira S, Arenillas JF, Coscojuela P, Romero F, Codina A. Thrombolysis-related hemorrhagic infarction: a marker of early reperfusion, reduced infarct size, and improved outcome in patients with proximal middle cerebral artery occlusion. *Stroke.* 2002;33:1551–1556.